Title

Direct Demonstration of Topological Stability of Magnetic Skyrmions via Topology Manipulation

Journal
ACS Nano, 14(3)

ISSN
1936-0851

Authors
Je, Soong-Geun
Han, Hee-Sung
Kim, Kwon
et al.

Publication Date
2020-03-24

DOI
10.1021/acsnano.9b08699

Peer reviewed

Direct Demonstration of Topological Stability of Magnetic Skyrmions *via* Topology Manipulation

Soong-Geun Je,[†,‡,§,∥] Hee-Sung Han,[¶] Se Kwon Kim,[**] Sergio A. Montoya,[††] Weilun Chao,[†] Ik-Sun Hong,[‡‡] Eric E. Fullerton,[§§,∥∥] Ki-Suk Lee,[¶] Kyung-Jin Lee,[‡‡,¶¶] Mi-Young Im,[†,‡,¶,*] and Jung-Il Hong[‡,*]

[†]Center for X-ray Optics, Lawrence Berkeley National Laboratory, Berkeley, CA 94720, USA.

[‡]Department of Emerging Materials Science, DGIST, Daegu 42988, Korea.

[§]Center for Spin-Orbitronic Materials, Korea University, Seoul 02841, Korea.

[∥]Department of Physics, Chonnam National University, Gwangju 61186, Korea

[¶]School of Materials Science and Engineering, Ulsan National Institute of Science and Technology, Ulsan 44919, Korea.

[**]Department of Physics and Astronomy, University of Missouri, Columbia, MO 65211, USA.

[††]Space and Naval Warfare Systems Center Pacific, San Diego, CA 92152, USA.

[‡‡]KU-KIST Graduate School of Converging Science and Technology, Korea University, Seoul 02841, Korea.

[§§]Center for Memory and Recording Research, University of California–San Diego, La Jolla, CA 92093, USA.

[∥∥]Department of Electrical and Computer Engineering, University of California–San Diego, La Jolla, CA 92093, USA.

[¶¶]Department of Materials Science and Engineering, Korea University, Seoul 02841, Korea.

*e-mail: mim@lbl.gov; jihong@dgist.ac.kr

Abstract

Topological protection precludes a continuous deformation between topologically inequivalent configurations in a continuum. Motivated by this concept, magnetic skyrmions, topologically nontrivial spin textures, are expected to exhibit the topological stability, thereby offering a prospect as a nanometer-scale non-volatile information carrier. In real materials, however, atomic spins are configured as not continuous but discrete distribution, which raises a fundamental question if the topological stability is indeed preserved for real magnetic skyrmions. Answering this question necessitates a direct comparison between topologically nontrivial and trivial spin textures, but the direct comparison in one sample under the same magnetic fields has been challenging. Here we report how to selectively achieve either a skyrmion state or a topologically trivial bubble state in a single specimen and thereby experimentally show how robust the skyrmion structure is in comparison with the bubbles. We demonstrate that topologically nontrivial magnetic skyrmions show longer lifetimes than trivial bubble structures, evidencing the topological stability in a real discrete system. Our work corroborates the physical importance of the topology in the magnetic materials, which has hitherto been suggested by mathematical arguments, providing an important step towards ever-dense and more-stable magnetic devices.

Keywords: topology manipulation, topological stability, topological protection, magnetic skyrmion, magnetic bubble, lifetime, FeGd

Topology[1,2] constitutes profound viewpoints in modern physics on revealing various robust states existing in many physical systems including topological insulators,[3,4] ultracold atoms,[5] topological insulator lasers[6] and topological mechanical metamaterials.[7] Topology has also been successful in representing various magnetic phenomena.[1,8-18] In a continuum description of magnetic systems, the topological protection means that a continuous deformation between spin structures with different topologies is not allowed.[1,2] This implies exceptional stability of spin textures with nontrivial topology against collapse to a uniform spin configuration.

A compelling example of such topological spin structures is the magnetic skyrmion. It is a swirling spin structure (Figure 1a) possessing a quantized topological charge defined by $Q=\frac{1}{4\pi}\int m\cdot(\partial_x m\times\partial_y m)\,dxdy=1$, which measures how many times m winds the unit sphere within a closed surface, where m is the unit vector of magnetization. In terms of topological charge, the skyrmion structure is topologically distinct from a uniform ferromagnetic state with $Q=0$, hence characterized as a topologically nontrivial spin texture.

It is anticipated that magnetic skyrmions with exceptionally small sizes remain robust and can be driven by electric currents easily without being interrupted or annihilated by system disorders such as structural defects.[19,28] Therefore, it is considered as a promising candidate for information carrier in the applications for ultrahigh density data storage,[19,20,29] logic,[30] and neuromorphic[31,32] technologies. As the successful implementation of skyrmion-based applications crucially relies on the retention of skyrmion structures, the topologically protected property of the skyrmions is the most important prerequisite.

In real materials, however, magnetic moments are localized on atoms in a discrete lattice that the collapse of magnetic skyrmions is plausible by overcoming a finite energy barrier in an atomistic length scale, where the topological argument is nullified. This realistic situation thus naturally raises fundamentally and technologically important questions: Is the topological protection still a viable concept to guarantee the skyrmion stability and how strong is the constraint in the real discrete system?

Considerable efforts have been devoted to addressing the issues on the skyrmion stability in a real system, but they still remain controversial.[33] Theoretical works have suggested that there are alternative skyrmion decay paths along which the energy barrier is lower than that of atomistic-shrinking of skyrmions[34-37] or the entropy has an important role in the skyrmion lifetime.[37-39] A few experimental works[40-42] have dealt with the skyrmion stability by measuring the lifetime. However, the lack of direct experimental comparison of topologically trivial and nontrivial spin structures under the identical environment such as within the same specimen leaves the issue of ambiguity because the skyrmion lifetime is highly dependent not only on the topological effect but also on other factors including material properties.

A representative of the topologically trivial counterpart to the skyrmion is a bubble of $Q=0$ as schematically depicted in Figure 1b. The boundary of a bubble consists of a pair of half circles with winding spins in the opposite direction and the two half circles are joined by Bloch lines. Since its topological charge Q equals to 0, the topological effect does not participate in the annihilation of the bubble.

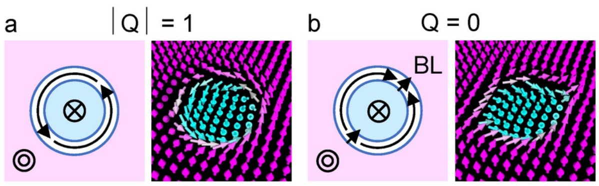

FIG. 1. *Schematic illustration of a topologically nontrivial skyrmion and a topologically trivial bubble.* (a) Bloch-type skyrmion with $|Q \vee ¿ 1$. (b) Bubble with $Q=0$. The BL refers to the Bloch line.

The experimental difficulties hindering a thorough assessment of the topological effect to the skyrmion stability is twofold. Firstly, experimental measurement of sub-100 nm spin structures with a sufficiently high temporal resolution to detect the skyrmion lifetime is technically a challenging issue. Secondly and more importantly, tailoring the topology,[43,44] thereby selectively preparing either skyrmions or bubbles in the same material, is another challenging issue that has not been fully explored. A measurable physical quantity to estimate the topological effect is the lifetime, which however varies drastically depending on material properties. Therefore, resolving the second issue is particularly important to directly compare the stabilities of topologically nontrivial and trivial structures on an equal footing.

Overcoming the two challenges mentioned above, we experimentally demonstrate the stability of magnetic skyrmions rooted in topology. By choosing different magnetic field pathways, we are able to selectively reach either a magnetic skyrmion state or a bubble state in the same specimen under the same magnetic field strength, providing a versatile route towards the topology manipulation and fair comparison of the topological effect. The lifetimes of both skyrmions and bubbles are then studied using the full-field transmission soft x-ray microscopy (MTXM) combined with pulsed magnetic fields of various durations to enhance the time resolution. We find that magnetic skyrmions exhibit much longer lifetime than bubbles even at higher fields. This result is in line with the expectation for the topological protection: the topology change is involved in the annihilation of skyrmions whereas it is not in the annihilation of bubbles. This work provides the experimental evidence for the existence of the topological stability of skyrmions in a real discrete system.

RESULTS AND DISCUSSIONS

For this study, the material we selected is an amorphous ferrimagnetic Fe/Gd multilayer film [Fe(0.34 nm)/Gd(0.4 nm)]×120. In a previous work,[45] Lorentz transmission electron microscopy and MTXM study confirmed that this material exhibits a dipolar-stabilized skyrmions with a flux-closure structure upon increasing out-of-plane (OOP) fields by pinching off stripe domains. Owing to the negligible Dzyaloshinskii-Moriya interaction, the skyrmions in this material are of Bloch type[45] around the middle layer of the film as shown in Figure 1a (see Supporting Information for the generation process and the structure of skyrmion in this material). Also, topologically trivial bubbles coexisting with skyrmions are often observed,[46] suggesting that this material is able to serve as an ideal testbed for the comparison of distinct topological structures.

We first explain how to achieve selective formation of either only skyrmions or only bubbles in a same specimen. Previous observations that bubbles are found in the presence of a small in-plane (IP) field[45-48] hint at the potential utility of an IP field for the selective realization of a skyrmion phase or a bubble phase. Here the role of the IP field is to stabilize the bubble structure (Figure 1b) in a way that aligns the spins of the bubble boundary along the IP field, and this has similarly been used to deform domain wall structures of microscale circular domains.[49-51] Given that skyrmions and bubbles are formed by pinching off stripe domains,[45-48] applying the IP field in the direction of the stripe domain wall magnetization could result in the formation of the bubbles. Conversely, if one of the half circles of the bubble boundary

(Figure 1b) is reversed by reversing the IP field, the skyrmion structures could be achieved instead.

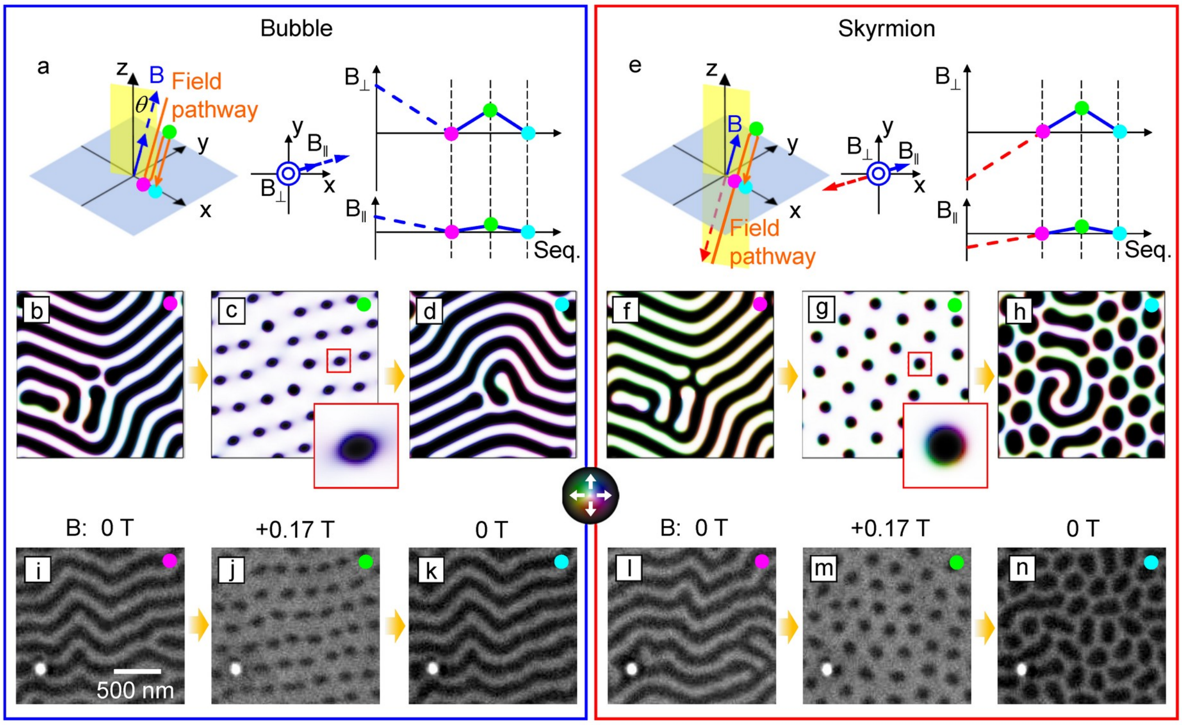

FIG 2. *Micromagnetic simulation and experimental results for the topology manipulation.* (a) Magnetic field geometry and pathway (orange solid line) for the bubble phase. (b-d) Simulation results taken at the colored circles along the pathway in (a). The applied magnetic field for (c) is +0.28 T and the inset shows the zoomed image for the bubble structure. (e) Magnetic field geometry and pathway (orange solid line) for the skyrmion phase. (f-h) Simulation results taken at the colored circles along the pathway in (e). The applied magnetic field for (g) is +0.28 T and the inset displays the zoomed image for the skyrmion structure. (i-k) Corresponding MTXM images obtained for the pathway (colored circles) for the bubble phase. (l-n) Corresponding MTXM images obtained for the pathway (colored circles) for the skyrmion phase. The white spot in (i-n) is a structural defect, confirming that the bubble state and the skyrmion state are obtained in the same position.

We corroborate the above idea by micromagnetic simulations with magnetic parameters for the Fe/Gd multilayer film (see Methods). Figure 2a,e schematically illustrate the designed pathways of the magnetic field B to realize the bubble phase and the skyrmion phase, respectively. The colored circles along the magnetic field pathways indicate the corresponding magnetic images which will be shown in a moment. Here, for all cases, the magnetic field B is slightly tilted away from the z-axis ($\theta = 1^\circ$) in order to utilize small IP fields $B_\parallel$. Initially, strong saturation fields (dotted arrows in Figure 2a,e) are applied and then the fields are reduced to zero. After the initializing field sequence, ordered stripe domains are obtained for both cases as shown in Figure 2b,e. Figure 2b,e present the magnetization of the middle layer and the in-plane magnetization of the domain walls is represented the colors according to the depicted color wheel. The colors show that there is a clear tendency for the in-plane magnetization to be aligned in the direction of the IP fields that had existed. Note that, in two different situations (Figure 2b,f), the initial saturation fields are in the opposite direction but have the same magnitude so that the resultant stripe phases are identical upon the reversal of the film.

The tilted field B is then increased until the stripe domains are pinched off. When the field is along the same direction as the saturation field and thus the direction of $B_{\parallel}$ does not change (Figure 2a), we obtain the bubble phase as expected (Figure 2c). On the other hand, when the magnetic field is in the opposite direction to the saturation field and hence the IP component $B_{\parallel}$ changes its direction accordingly (Figure 2e), we obtain the skyrmion phase of $|Q|=1$, as shown in Figure 2g. It is worth noting that completely different topological phases are obtained from basically the same initial stripe domain phase by following different IP field histories, suggesting the feasibility of the topology manipulation. Their topological difference can also be highlighted when the magnetic field is brough to zero. The bubble state (Figure 2c) returns to an ordered stripe domain state (Figure 2d) by connecting the bubbles in line. However, the skyrmions (Figure 2g) are topologically not allowed to merge, conserving their isolated features (Figure 2h) even at zero field.[28]

To experimentally confirm the above predictions, we investigate the Fe/Gd multilayered film at room temperature using the MTXM[52] at the Advanced Light Source (XM-1, BL6.1.2), Lawrence Berkeley National Laboratory (see Methods). We follow the tilted magnetic field pathways as described above. Figure 2i-k and Figure 2l-n correspond to the magnetic images obtained along the field pathways for the bubble case and the skyrmion case, respectively. For both cases, the ordered stripe phases are obtained at zero field (Figure 2i,l).

When the field B increases to +0.17 T, however, the final states are different from each other even at the same magnetic field (Figure 2j,m). Although isolated domains cover the entire film area for both cases, the shape of individual domains are slightly different. Figure 2m shows circular domains of ~90 nm in diameter whereas Figure 2j shows elongated domains. These results are in good agreement with the micromagnetic simulations (Figure 2c,g), confirming that the bubble phase and the skyrmion phase are selectively realized in the single specimen. It should also be emphasized that the two distinct phases are obtained at the same magnetic field, enabling a fair comparison of the topological characteristics between the two topologically distinct phases. Furthermore, the images taken when the field is brought to zero (Figure 2k,n) coincide with the simulation results (Figure 2d,h), more supporting that Figure 2j and Figure 2m are the bubble and skyrmion phases, respectively.

Having established the two topologically inequivalent phases in the same specimen, we investigate their topological stabilities upon increasing the external magnetic field B which causes those structures to shrink. In all the following experiments, the same magnetic field geometry (tilted field with $\theta = 1^{\circ}$) is used, and therefore a small IP field $B_{\parallel}$ exists (~1.7 % of the perpendicular field $B_{\perp}$). We mention, however, that the presence of the $B_{\parallel}$ does not change the general conclusion of this work because of the very small $B_{\parallel}$ (for a relevant discussion, see Supporting Information).

We first study how differently the topologically distinct spin textures persist upon increasing the external magnetic field B. As respectively shown in Figure 3a,b, the sizes of both bubbles and skyrmions reduce as the magnetic field increases, and they begin to disappear as the field is further increased. The normalized number of skyrmions (bubbles) n_N, remaining number divided by its initial number after the field application, and the radius of skyrmions (bubbles) as a function of the magnetic field B are summarized in Figure 3c,d, respectively. Here the radius of elliptical bubbles is defined as the radius of a circle that has the same area of an ellipse. Two interesting aspects can be underlined. First, the number of skyrmions decreases much slower than that of bubbles. Second, upon increasing the applied field, a skyrmion survives to a much smaller size than a bubble. The size of skyrmion continuously decreases down to ~25 nm, whereas the bubble size decreases slowly to ~35 nm before the bubbles abruptly disappear. Considering the general correlation between the stability and the achievable minimum size, this result clearly shows superior stability of skyrmions to bubbles.

These results can be explained by the topological effect. The transformation of bubbles into a uniformly magnetized state is a continuous change of the spin structure that occurs within the same topological sector. However, the collapse of skyrmions into a uniform state requires a topological change, making the skyrmions persist at much stronger fields. Thus, the stronger field for the skyrmion annihilation corresponds to the extra field required to break the topology of the skyrmion structure. The topological change and corresponding extra field involve a rapid increase of the exchange-energy density at a Bloch point,[11,15,35] which is a topologically-originated high energy barrier corresponding to the length scale of lattice constant, *i.e.*, ultraviolet energy-cutoff between them, in continuum systems.[53] In real discrete systems, the increased exchange energy is finite,[8,14,16] but still large enough to guarantee a better stability for skyrmions than bubbles. A relevant discussion on the energetics of the skyrmion and bubble with respect to the increasing magnetic field can also be found in Supporting Information.

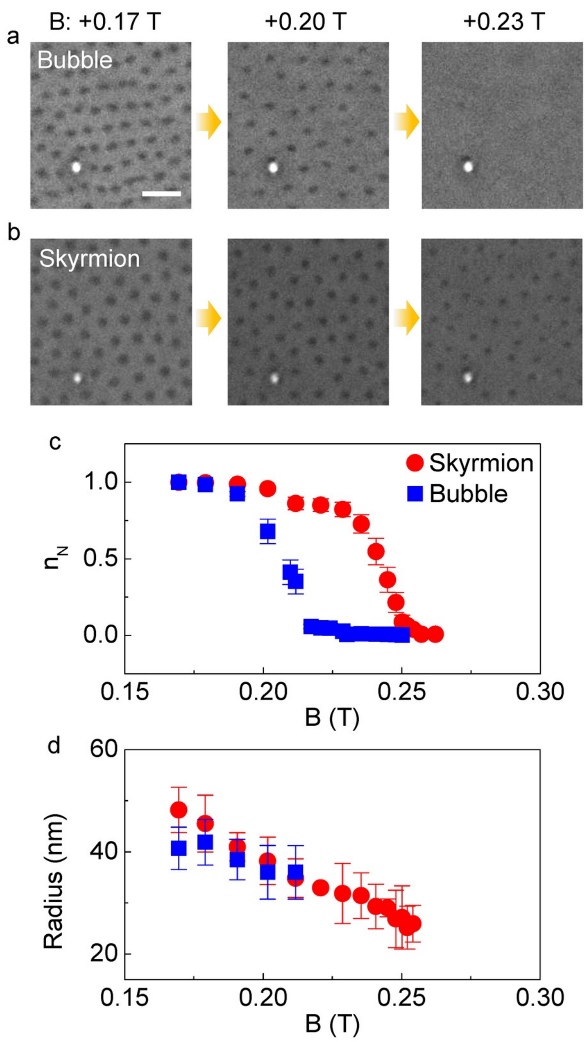

FIG. 3. *Magnetic field dependence of the bubble and the skyrmion phases.* (a) Evolution of the bubble phase with increasing fields. The scale bar is 500 nm. (b) Evolution of the skyrmion phase with increasing fields. (c) Annihilation of bubbles and skyrmions as a function of the magnetic field. The n_N is the normalized number of spin structures which is divided by its initial number of spin textures. (d) Radius of bubbles and skyrmions as a

function of the magnetic field.

The topological stability is further supported by the significantly longer lifetimes of skyrmions than those of bubbles. The lifetime τ is directly related to the free energy barrier ΔF, given as[40] $\tau(B)=\tau_{00}e^{\Delta F(B)/k_BT}$, where the prefactor τ_{00} is the characteristic time, $\Delta F=\Delta E-T\Delta S$, and the k_BT is the thermal energy which is the product of the Boltzmann constant k_B and temperature T. Here, ΔE and ΔS are the activation energy and entropy differences between the metastable state and the saddle point. In our cases where plenty of identical topological structures are present, the lifetime is represented by the decay of the number of spin textures with time.

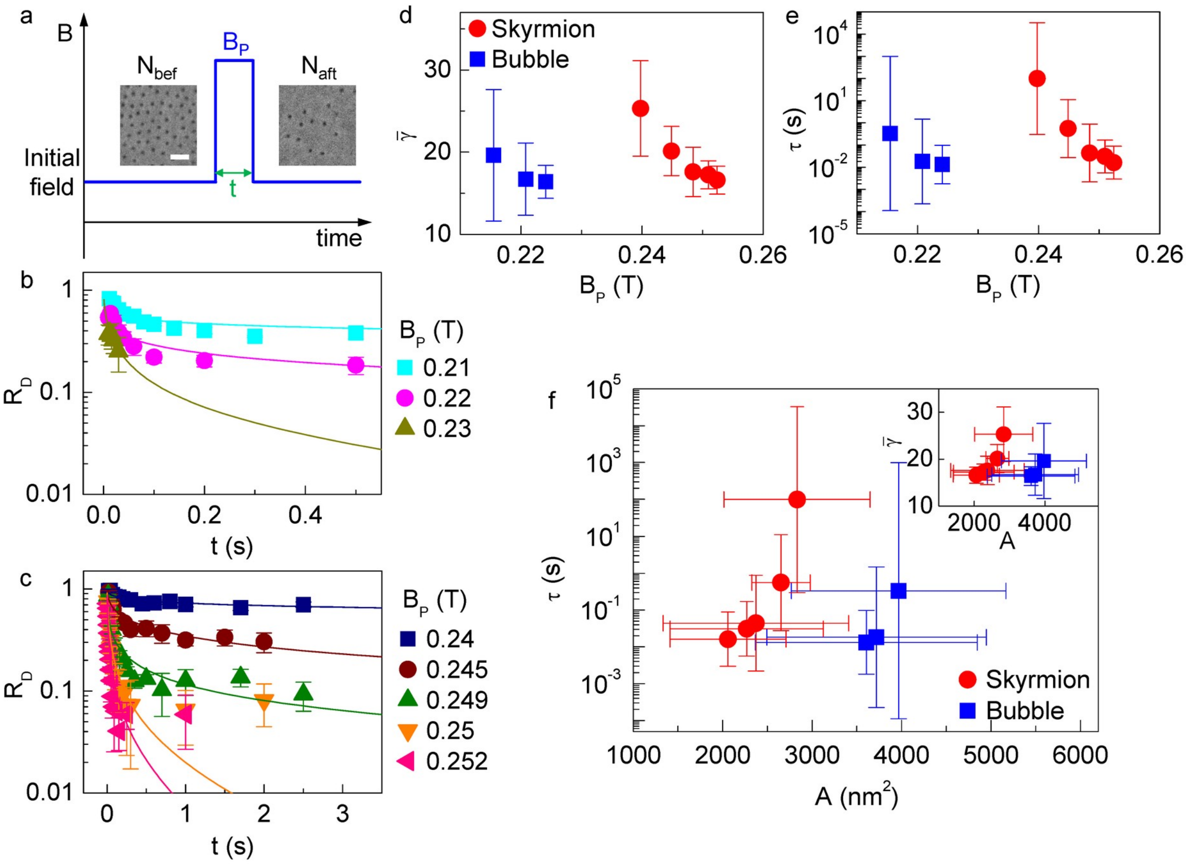

FIG. 4. *Time evolution of the decays of bubbles and skyrmions*. (a) Schematic of the experiment for the decay during the pulsed magnetic field B_P. The scale bar is 500 nm. (b,c) The decay rate R_D of bubbles (b) and skyrmions (c) with respect to the duration t. Measured data points were fitted based on the exponential relationship and plotted in solid lines. (d,e) The reduced free energy barrier $\acute{\gamma}$ (d) and the lifetime τ (e) with respect to the field B_P. (f) The lifetime τ of bubbles and skyrmions as a function of their areas A. The inset shows the corresponding $\acute{\gamma}$ with respect to the area A. Red circles (blue squares) correspond the skyrmion (bubble). The error bars for $\acute{\gamma}$ and τ are determined by the standard deviation σ.

To achieve a better temporal resolution, we apply a pulsed magnetic field B_P as illustrated in Figure 4a, including typical magnetic images before and after the pulse field application. Either the skyrmion phase or the bubble phase is prepared under the initial field of +0.2 T, and the number of spin structures is counted (N_{bef}). A pulsed magnetic field B_P is applied subsequently, and then the number of spin structures (N_{aft}) is counted again. It is confirmed that the initial field does not initiate the decay of spin textures, and the natural nucleation does not occur when the field comes back to the initial field level after the pulse field B_P. This guarantees that the decay events proceed only during the presence of the pulsed magnetic field B_P, thereby allowing us to estimate the decay rate with time by changing the duration t of the B_P. The minimum duration which ensures a well-defined magnetic pulse shape is ~20 ms (see Methods). The decay rate R_D is calculated by dividing the N_{aft} by the N_{bef}, and the initial state for N_{bef} is always initialized every time before the application of the B_P. For statistical significance, spin textures of N_{bef} > 100 in one area are analyzed, and R_D is averaged over 4 different areas in the film to obtain a single data point in Figure 4.

Figure 4b,c summarize the decay rates R_D's of bubbles and skyrmions under various magnetic fields as a function of time, respectively. The decay rate R_D rapidly decreases with time in line with the previous work by Wild *et al.*,[40] where an exponential time dependence of the skyrmion decaying process was observed. We fit the data (solid lines) by the exponential equation $R_D(t)=\int_0^{\infty} \frac{1}{\sqrt{2\pi\sigma^2}} \exp\left[\frac{-(\gamma-\acute{\gamma})^2}{2\sigma^2}\right] \exp\left[\frac{-t}{\tau_{00}\exp(\gamma)}\right] d\gamma$, where the γ ($\acute{\gamma}$) stands for the reduced free energy barrier $\Delta F/k_B T$ (mean value of the γ), the σ is the standard deviation of γ and the τ_{00} is assumed to be 10^{-9} s. Gaussian distribution of γ is assumed to account for the local variation of the magnetic properties in the sputtered film and consequently to improve the fit.

The obtained free energy barrier $\acute{\gamma}$ and the corresponding τ, which is converted from $\acute{\gamma}$using the Arrhenius law, are respectively shown in Figure 4d,e. Note that, while the $\acute{\gamma}$ is extracted under the assumption of the fixed τ_{00}, the reconstructed τ does not contain any uncertainty which arises from the presumed τ_{00}. Since the skyrmion decay occurs in a much stronger field range than the bubble case, the lifetimes could not be compared at the same magnetic fields.

However, one can easily infer that the lifetime τ of skyrmions is much greater than that of the bubbles even at much stronger magnetic fields, in agreement with the result in Figure 3c.

The enhanced stability of skyrmions can also be highlighted when the τ is plotted as a function of the size (area, A) as shown in Figure 4f. Here, A is calculated based on the data in Figure 3d, and linear extrapolation is adopted for the bubble area as the radius cannot be measured due to the fast annihilation of the bubbles. For both skyrmions and bubbles, it is noticed that the lifetime τ increases as the A becomes larger, which is consistent with the general expectation that larger objects are more stable.[1,34] The most salient feature in Figure 4f is that skyrmions (red circles) display much longer τ than bubbles (blue squares) despite their smaller sizes even at stronger fields, clearly indicating that the topological protection works for skyrmions, but not for bubbles. This also highlights the viability of magnetic skyrmions as topologically protected information carriers. The free energy barrier, $\acute{\gamma}$, with respect to the size is also presented in the inset of Figure 4f. The greater $\acute{\gamma}$ as well as the smaller sizes of skyrmions indicates that there is an additional factor associated with the topological change in skyrmion annihilation. Several works[37-41] have recently pointed out that entropic effect has an important role in the lifetime of skyrmions. In our present work, we are unable to separate the free energy barrier ΔF into the activation energy barrier ΔE and the entropy ΔS. However, it does not alter our main conclusion; topological magnetic skyrmions have longer lifetimes and thus more stable than non-topological bubbles. The detailed separation between the energy barrier effect and the entropy effect would require temperature-dependent measurements,[40] which is beyond the scope of this work.

CONCLUSIONS

To date, magnetic skyrmions have been the focus of extensive research because of the expectation for the exceptional stability rooted in topology. This most important prerequisite of the skyrmion has always been taken for granted without rigorous experimental confirmation. Also, as another great challenge to harness the topological nature of the materials, an efficient and versatile way to control the topology of the system has been elusive. In the present work, we experimentally demonstrate that the topology of final states evolved from the same initial state can be controlled by following different pathways, enabling the manipulation of the topology in a given material system. This ability to control the topology of magnets would allow dynamic manipulation of various transport properties, *e.g.*, Hall resistance which will be enhanced only in the skyrmion phase due to the topological Hall effect. By exploiting the revealed topology control, we demonstrate the existence of topological stability that has been often doubted in realistic discrete systems. We expect that our finding initiates further research efforts to tailor the topology of the system and enhance the topological energy barrier, which will facilitate the realization of ultrahigh density devices using topological spin structures.

METHODS

Sample Preparation and Imaging Technique. The amorphous Fe/Gd multilayer film was grown by magnetron sputtering at room temperature in a 3 mTorr Ar pressure at a base pressure of <3×10^{-8} Torr. Fe and Gd layers were alternatively deposited on a 100 nm thick X-ray transparent Si_3N_4 membrane substrate and the process was repeated until the desired repetition number of 120 was achieved. The perpendicular magnetic contrast was measured by the X-ray magnetic circular dichroism (XMCD) at the Fe L_3 (708 eV) absorption edge in perpendicular geometry where the film surface is normal to the X-ray propagation direction. XMCD images were acquired using full-field magnetic transmission soft X-ray microscopy (MTXM) at the Advanced Light Source, Lawrence Berkeley National Laboratory (XM-1, beamline 6.1.2).

Micromagnetic Simulations. Micromagnetic simulations were performed using the MuMax^3 code.[54] The model system was a $1{,}500\times1{,}500\times80$ nm^3 plate with mesh sizes of $5\times5\times5$ nm^3. For the simulations, typical magnetic parameters for the amorphous Fe/Gd ferrmimagnet,[45] *i.e.*, a saturation magnetization $M_S = 4\times10^5$ A/m, a uniaxial anisotropy $K_U = 4\times10^4$ J/m^3, and an exchange constant $A_{ex} = 5\times10^{-12}$ J/m, are used.

Pulsed Magnetic Field. The minimum reliable duration of the pulsed magnetic field with a well-defined shape was confirmed by monitoring the current flowing through the coil for the magnetic field. The actual current pulse shape was measured by detecting the voltage across a test resistor of 0.5 Ω which is connected to the coil in series. As the resistance is sufficiently smaller than the resistance of the coil (8 Ω), the interference by the test resistor connection can be minimized. The detected voltage representing the current pulse profile for various durations (Figure S3, Supporting Information) guarantees that the control of the duration is reliable.

ACKNOWLEDGMENTS

Works at the ALS were supported by U.S. Department of Energy (DE-AC02-05CH11231). SGJ, KJL and JIH acknowledges the support from the Future Materials Discovery Program through the NRF-2015M3D1A1070465. JIH and KSL also acknowledge the support from NRF-2017R1A2B4003139 and NRF-2019R1A2C2002996. SKK was supported by the start-up fund at the University of Missouri.

1

REFERENCES

1. Braun, H.-B. Topological effects in nanomagnetism: From superparamagnetism to chiral quantum solitons. *Adv. Phys.* **2012**, **61**, 1-116.
2. Schwarz, A. S. *Topology for Physicists*; Schwarz, A. S., Eds.; Springer-Verlag: Berlin/ Heidelberg, 1994.
3. Chen, Y. L.; Chu, J.-H.; Analytis, J. G.; Liu, Z. K.; Igarashi, K.; Kuo, H. H.; Qi, X. L.; Mo, S. K.; Moore, R. G.; Lu, D. H.; Hashimoto, M.; Sasagawa, T.; Zhang, S. C.; Fisher, I. R.; Hussain, Z.; Shen, Z. X. Massive Dirac Fermion on the Surface of a Magnetically Doped Topological Insulator. *Science* **2010**, 329, 659–662.
4. Bernevig, B. A.; Hughes, T. L.; Zhang, S. C. Quantum Spin Hall Effect and Topological Phase Transition in HgTe Quantum Wells. Science **2006**, 314, 1757–1761.
5. Jotzu, G.; Messer, M.; Desbuquois, R.; Lebrat, M.; Uehlinger, T.; Greif, D.; Esslinger, T. Experimental Realisation of the Topological Haldane Model, *Nature* **2014**, 515, 237–240.
6. Bandres, M. A.; Wittek, S.; Harari, G.; Parto, M.; Ren, J.; Segev, M.; Christodoulides, D. N.; Khajavikhan, M. Topological Insulator Laser: Experiments. *Science* **2018**, 359, eaar4005.
7. Nash, L. M.; Kleckner, D.; Read, A.; Vitelli, V.; Turner, A. M.; Irvine, W. T. M. Topological Mechanics of Gyroscopic Metamaterials. *Proc. Natl. Acad. Sci. U. S. A.* **2015**, 112, 14495–14500.
8. Tretiakov, O. A.; Tchernyshyov, O. Vortices in Thin Ferromagnetic Films and the Skyrmion Number. *Phys. Rev. B: Condens. Matter Mater. Phys.* **2007**, 75, 012408.
9. Yoshimura, Y.; Kim, K.-J.; Taniguchi, T.; Tono, T.; Ueda, K.; Hiramatsu, R.; Moriyama, T.; Yamada, K.; Nakatani, Y.; Ono, T. Soliton-like Magnetic Domain Wall Motion Induced by the Interfacial Dzyaloshinskii–Moriya Interaction. *Nat. Phys.* **2016**, 12, 157–161.
10. Im, M.-Y.; Han, H.-S.; Jung, M.-S.; Yu, Y.-S.; Lee, S.; Yoon, S.; Chao, W.; Fischer, P.; Hong, J.-I.; Lee, K.-S. Dynamics of the Bloch Point in an Asymmetric Permalloy Disk. *Nat. Commun.* **2019**, 10, 593.
11. Milde, P.; Köhler, D.; Seidel, J.; Eng, L. M.; Bauer, A.; Chacon, A.; Kindervater, J.; Mühlbauer, S.; Pfleiderer, C.; Buhrandt, S.; Schütte, C.; Rosch, A. Unwinding of a Skyrmion Lattice by Magnetic Monopoles. *Science* **2013**, 340, 1076–1080.
12. Charilaou, M.; Braun, H.-B.; Löffler, J. F. Monopole-Induced Emergent Electric Fields in Ferromagnetic Nanowires. *Phys. Rev. Lett.* **2018**, 121, 097202.
13. Yin, G.; Li, Y.; Kong, L.; Lake, R. K.; Chien, C. L.; Zang, J. Topological Charge

Analysis of Ultrafast Single Skyrmion Creation. *Phys. Rev. B: Condens. Matter Mater. Phys.* **2016**, 93, 174403.

14. Thiaville, A. García, J. M.; Dittrich, R.; Miltat, J.; Schrefl, T. Micromagnetic Study of Bloch-Point-Mediated Vortex Core Reversal, *Phys. Rev. B: Condens. Matter Mater. Phys.* **2003**, 67, 094410.

15. Schütte, C.; Rosch, A. Dynamics and Energetics of Emergent Magnetic Monopoles in Chiral Magnets. *Phys. Rev. B: Condens. Matter Mater. Phys.* **2014**, **90**, 174432.

16. Kim, S. K.; Tchernyshyov, O. Pinning of a Bloch Point by an Atomic Lattice. *Phys. Rev. B: Condens. Matter Mater. Phys.* **2013**, 88, 174402.

17. Jiang, W.; Zhang, X.; Yu, G.; Zhang, W.; Wang, X.; Jungfleisch, M. B.; Pearson, J. E.; Cheng, X.; Heinonen, O.; Wang, K. L.; Zhou, Y.; Hoffmann, A.; te Velthuis, S. G. E. Direct Observation of the Skyrmion Hall Effect. *Nat. Phys.* **2016**, 13, 162–169.

18. Litzius, K.; Lemesh, I.; Krüger, B.; Bassirian, P.; Caretta, L.; Richter, K.; Büttner, F.; Sato, K.; Tretiakov, O. A.; Förster, J.; Reeve, R. M.; Weigand, M.; Bykova, I.; Stoll, H.; Schütz, G.; Beach, G. S. D.; Kläui, M. Skyrmion Hall Effect Revealed by Direct Time-Resolved X-Ray Microscopy. *Nat. Phys.* **2016**, 13, 170–175.

19. Sampaio, J.; Cros, V.; Rohart, S.; Thiaville, A.; Fert, A. Nucleation, Stability and Current-Induced Motion of Isolated Magnetic Skyrmions in Nanostructures. *Nat. Nanotechnol.* **2013**, 8, 839–844.

20. Fert, A.; Cros, V.; Sampaio, J. Skyrmions on the Track. *Nat. Nanotechnol.* **2013**, 8, 152–156.

21. Nagaosa, N.; Tokura, Y. Topological Properties and Dynamics of Magnetic Skyrmions. *Nat. Nanotechnol.* **2013**, 8, 899–911.

22. Boulle, O.; Vogel, J.; Yang, H.; Pizzini, S.; de Souza Chaves, D.; Locatelli, A.; Menteş, T. O.; Sala, A.; Buda-Prejbeanu, L. D.; Klein, O.; Belmeguenai, M.; Roussigné, Y.; Stashkevich, A.; Chérif, S. M.; Aballe, L.; Foerster, M.; Chshiev, M.; Auffret, S.; Miron, I. M.; Gaudin, G. Room-Temperature Chiral Magnetic Skyrmions in Ultrathin Magnetic Nanostructures. *Nat. Nanotechnol.* **2016**, 11, 449–454.

23. Woo, S.; Litzius, K.; Krüger, B.; Im, M.-Y.; Caretta, L.; Richter, K.; Mann, M.; Krone, A.; Reeve, R. M.; Weigand, M.; Agrawal, P.; Lemesh, I.; Mawass, M.-A.; Fischer, P.; Kläui, M.; Beach, G. S. D. Observation of Room Temperature Magnetic Skyrmions and their Current-Driven Dynamics in Ultrathin Co Films. *Nat. Mater.* **2016**, 15, 501–506.

24. Hrabec, A.; Sampaio, J.; Belmeguenai, M.; Gross, I.; Weil, R.; Chérif, S. M.; Stashkevich, A.; Jacques, V.; Thiaville, A.; Rohart, S. Current-Induced Skyrmion Generation and Dynamics in Symmetric Bilayers. *Nat. Commun.* **2017**, 8, 15765.

25. Caretta, L.; Mann, M.; Büttner, F.; Ueda, K.; Pfau, B.; Günther, C. M.; Hessing, P.; Churikova, A.; Klose, C.; Schneider, M.; Engel, D.; Marcus, C.; Bono, D.; Bagschik, K.; Eisebitt, S.; Beach, G. S. D. Fast Current-Driven Domain Walls and Small Skyrmions in a Compensated Ferrimagnet. *Nat. Nanotechnol.* **2018**, 13, 1154–1160.

26. Romming, N.; Kubetzka, A.; Hanneken, C.; von Bergmann, K.; Wiesendanger, R. Field-Dependent Size and Shape of Single Magnetic Skyrmions. *Phys. Rev. Lett.* **2015**, 114, 177203.

27. Iwasaki, J.; Mochizuki, M.; Nagaosa, N. Current-Induced Skyrmion Dynamics in Constricted Geometries. *Nat. Nanotechnol.* **2013**, 8, 742–747.

28. Je, S.-G.; Vallobra, P.; Srivastava, T.; Rojas-Sánchez, J.-C.; Pham, T. H.; Hehn, M.; Malinowski, G.; Baraduc, C.; Auffret, S.; Gaudin, G.; Mangin, S.; Béa, H.; Boulle, O. Creation of Magnetic Skyrmion Bubble Lattices by Ultrafast Laser in Ultrathin Films. *Nano Lett.* **2018**, 18, 7362–7371.

29. Tomasello, R.; Martinez, E.; Zivieri, R.; Torres, L.; Carpentieri, M.; Finocchio, G. A Strategy for the Design of Skyrmion Racetrack Memories. *Sci. Rep.* **2014**, 4, 6784.

30. Zhang, X.; Ezawa, M.; Zhou, Y. Magnetic Skyrmion Logic Gates: Conversion, Duplication and Merging of Skyrmions. *Sci. Rep.* **2015**, 5, 9400.

31. Prychynenko, D.; Sitte, M.; Litzius, K.; Krüger, B.; Bourianoff, G.; Kläui, M.; Sinova, J.; Everschor-Sitte, K. Magnetic Skyrmion as a Nonlinear Resistive Element: a Potential Building Block for Reservoir Computing. *Phys. Rev. Appl.* **2018**, 9, 014034.

32. Pinna, D.; Abreu Araujo, F.; Kim, J.-V.; Cros, V.; Querlioz, D.; Bessiere, P.; Droulez, J.; Grollier, J. Skyrmion Gas Manipulation for Probabilistic Computing, *Phys. Rev. Appl.* **2018**, 9, 064018.

33. Büttner, F.; Lemesh, I.; Beach, G. S. D. Theory of Isolated Magnetic Skyrmions: from Fundamentals to Room Temperature Applications, *Sci. Rep.* **2018**, 8, 4464.

34. Rohart, S.; Miltat, J.; Thiaville, A. Path to Collapse for an Isolated Néel Skyrmion. *Phys. Rev. B: Condens. Matter Mater. Phys.* **2016**, 93, 214412.

35. Cortés-Ortuño, D.; Wang, W.; Beg, M.; Pepper, R. A.; Bisotti, M.-A.; Carey, R.; Vousden, M.; Kluyver, T.; Hovorka, O.; Fangohr, H. Thermal Stability and Topological Protection of Skyrmions in Nanotracks. *Sci. Rep.* **2017**, **7**, 4060.

36. Stosic, D.; Mulkers, J.; Van Waeyenberge, B.; Ludermir, T. B.; Milošević, M. V. Paths to Collapse for Isolated Skyrmions in Few-Monolayer Ferromagnetic Flms. *Phys. Rev. B: Condens. Matter Mater. Phys.* **2017**, 95, 214418.

37. Bessarab, P. F.; Müller, G. P.; Lobanov, I. S.; Rybakov, F. N.; Kiselev, N. S.; Jónsson, H.; Uzdin, V. M.; Blügel, S.; Bergqvist, L.; Anna, D. Lifetime of Racetrack Skyrmions. *Sci. Rep.* **2018**, 8, 3433.

38. von Malottki, S.; Bessarab, P. F.; Haldar, S.; Delin, A.; Heinze, S. Skyrmion lifetime in ultrathin films. *Phys. Rev. B: Condens. Matter Mater. Phys.* **2019**, 99, 064409(R).

39. Desplat, D.; Suess, D.; Kim, J.-V.; Stamps, R. L. Thermal Stability of Metastable Magnetic Skyrmions: Entropic Narrowing and Significance of Internal Eigenmodes. *Phys. Rev. B: Condens. Matter Mater. Phys.* **2018**, 98, 134407.

40. Wild, J.; Meier, T. N. G.; Pöllath, S.; Kronseder, M.; Bauer, A.; Chacon, A.; Halder, M.; Schowalter, M.; Rosenauer, A.; Zweck, J.; Müller, J.; Rosch, A.; Pfleiderer, C.; Back, C. H. Entropy-Limited Topological Protection of Skyrmions. *Sci. Adv.* **2017**, 3, e1701704.

41. Hagemeister, J.; Romming, N.; von Bergmann, K.; Vedmedenko, E. Y.; Wiesendanger, R. Stability of Single Skyrmionic Bits, *Nat. Commun.* **2015**, 6, 8455.

42. Oike, H.; Kikkawa, A.; Kanazawa, N.; Taguchi, Y.; Kawasaki, M.; Tokura, Y.; Kagawa, F. Interplay Between Topological and Thermodynamic Stability in a Metastable Magnetic Skyrmion Lattice. *Nat. Phys.* **2016**, 12, 62–67.

43. Li, J.; Tan, A.; Moon, K.-W.; Doran, A.; Marcus, M. A.; Young, A. T.; Arenholz, E.; Ma, S.; Yang, R. F.; Hwang, C.; Qiu, Z. Q. Tailoring the Topology of an Artificial Magnetic Skyrmion. *Nat. Commun.* **2014**, 5, 4704.

44. Gilbert, D. A.; Maranville, B. B.; Balk, A. L.; Kirby, B. J.; Fischer, P.; Pierce, D. T.; Unguris, J.; Borchers, J. A.; Liu, K. Realization of Ground-State Artificial Skyrmion Lattices at Room Temperature. *Nat. Commun.* **2015**, 6, 946.

45. Montoya, S. A.; Couture, S.; Chess, J. J.; Lee, J. C. T.; Kent, N.; Henze, D.; Sinha, S. K.; Im, M.-Y.; Kevan, S. D.; Fischer, P.; McMorran, B. J.; Lomakin, V.; Roy, S.; Fullerton, E. E. Tailoring Magnetic Energies to Form Dipole Skyrmions and Skyrmion Lattices, *Phys. Rev. B: Condens. Matter Mater. Phys.* **2017**, 95, 24415.

46. Chess, J.; Montoya, S.; Lee, J.; Roy, S.; Kevan, S.; Fullerton, E.; McMorran, B. Observation of Skyrmions at Room-temperature in Amorphous Fe/Gd Films. *Microsc. Microanal.* **2015**, 21, 1649-1650.

47. Yu, X.; Mostovoy, M.; Tokunaga, Y.; Zhang, W.; Kimoto, K.; Matsui, Y.; Kaneko, Y.; Nagaosa, N.; Tokura, Y. Magnetic stripes and skyrmions with helicity reversals. *Proc. Natl. Acad. Sci. U. S. A.* **2012**, 109, 8856–8860.

48. Nagaosa, N.; Yu, X. Z.; Tokura, T. Gauge Fields in Real and Momentum Spaces in Magnets: Monopoles and Skyrmions. *Philos. Trans. R. Soc., A* **2012**, 370, 5806–5819.

49. Jiang, W. J.; Upadhyaya, P.; Zhang, W.; Yu, G. Q.; Jungfleisch, M. B.; Fradin, F. Y.; Pearson, J. E.; Tserkovnyak, Y.; Wang, K. L.; Heinonen, O.; te Velthuis, S. G. E.; Hoffmann, A. Blowing Magnetic Skyrmion Bubbles. *Science* **2015**, 349, 283–286.

50. Lee, O. J.; Liu, L. Q.; Pai, C. F.; Li, Y.; Tseng, H. W.; Gowtham, P. G.; Park, J. P.; Ralph, D. C.; Buhrman, R. A. Central Role of Domain Wall Depinning for

Perpendicular Magnetization Switching Driven by Spin Torque from the Spin Hall Effect. *Phys. Rev. B: Condens. Matter Mater. Phys.* **2014**, 89, 024418.

51. Je, S.-G.; Kim, D.-H.; Yoo, S.-C.; Min, B.-C.; Lee, K.-J.; Choe, S.-B. Asymmetric Magnetic Domain-Wall Motion by the Dzyaloshinskii-Moriya Interaction. *Phys. Rev. B: Condens. Matter Mater. Phys.* **2013**, 88, 214401.

52. Chao, W.; Hartneck, B. D.; Liddle, J. A.; Anderson, E. H.; Attwood, D. T. Soft X-ray Microscopy at a Spatial Resolution Better Than 15nm, *Nature* **2005**, 435, 1210–1213.

53. Heil, B.; Rosch, A.; Masell, J. Universality of Annihilation Barriers of Large Magnetic Skyrmions in Chiral and Frustrated Magnets. *Phys. Rev. B: Condens. Matter Mater. Phys.* **2019**, 100, 134424.

54. Vansteenkiste, A.; Leliaert, J.; Dvornik, M.; Helsen, M.; Garcia-Sanchez, F.; Van Waeyenberge, B. The Design and Verification of MuMax3, *AIP Adv.* **2014**, 4, 107133.